www.sciencemag.org/content/349/6254/1310/suppl/DC1

Supplementary Materials for

An ultrathin invisibility skin cloak for visible light

Xingjie Ni, Zi Jing Wong, Michael Mrejen, Yuan Wang, Xiang Zhang*

*Corresponding author. E-mail: xiang@berkeley.edu

Published 18 September 2015, *Science* **349**, 1310 (2015)
DOI: 10.1126/science.aac9411

This PDF file includes:

Materials and Methods

Fabrication method

The fabrication procedure (Fig. S1) begins with a 1 μm thick oxidation on a silicon substrate. A Gallium-based focused ion beam (FIB, FEI Strata 201) is then used to carve out the arbitrary-shaped three-dimensional profile and pattern the alignment marks. The oxidation layer is to trap and prevent the remnant Gallium ions (implanted during the FIB milling process) from diffusing to the top surface and causing undesired roughness. This is followed by electron beam evaporation of a 200-nm-thick layer of gold to form the bottom reflective layer. Next, we utilize an atomic force microscopy (AFM, Digital Instruments D3100) to map out the height profile of the entire three-dimensional object. Using the height data as the input, this allows us to design and fabricate the corresponding metasurface nanoantennas at each local position. An extra step of coordinate marking of the patterned alignment marks is also performed to further improve the alignment accuracy. We then do electron beam evaporation of a 50-nm thick MgF_2 layer to create the dielectric spacer for the gap plasmon resonance. Importantly, the metasurface nanoantennas are patterned on a bilayer PMMA A2 resist using electron beam lithography (EBL, Crestec CABL-9510CC) with extremely precise alignment. Upon development, a 2-nm Chromium adhesion layer and 30-nm gold layer are evaporated followed by the standard lift-off process.

Simulation method

The full-wave simulation for the three-dimensional invisibility skin cloak structure is done using a commercial finite element solver package – COMSOL Multiphysics. The arbitrarily-shaped object is first generated in MATLAB and then imported into COMSOL. The experimentally obtained optical constant of gold from Johnson and Christy *(46)* is used for the modeling of the gold nanoantennas and the back reflector. The refractive index of the spacer layer (MgF_2) is chosen to be 1.38. The scattered field formulation is used to calculate the reflected field. Perfectly matched layers (PMLs) are applied on all sides of the simulation domain to reduce the scattering from the sides. Scattering boundary condition is used behind the PMLs. Tetrahedral mesh elements are used and the element size is manually controlled to be smaller than 1/13 of the wavelength.

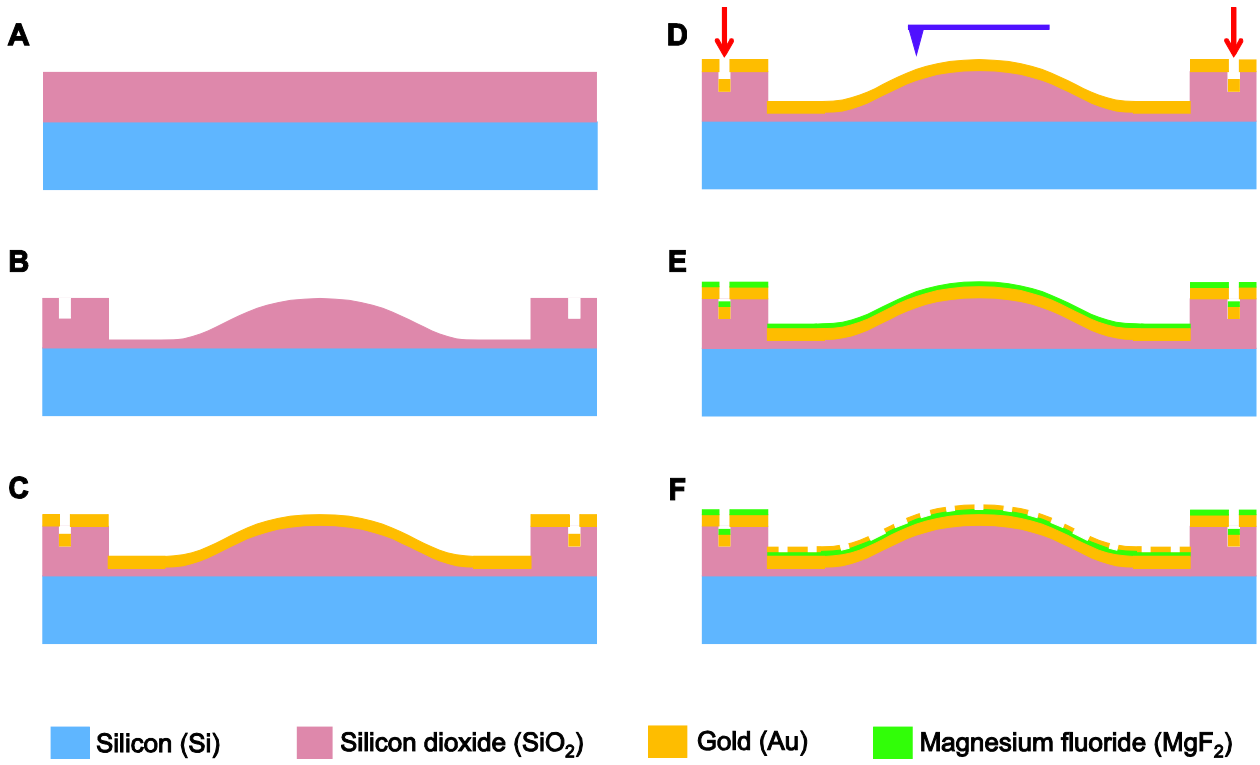

Figure S1. Schematic illustration of the fabrication process of the metasurface skin cloak device. (**A**) About 1 μm thick SiO_2 layer is formed on the Si substrate. (**B**) FIB milling of the three-dimensional profile together with the alignment marks. (**C**) Electron beam evaporation of a 200-nm-thick Au layer. (**D**) AFM scanning and coordinate marking of the alignment marks. (**E**) Electron beam evaporation of a 50-nm-thick MgF_2 layer. (**F**) EBL patterning of the metasurface nanostructures.

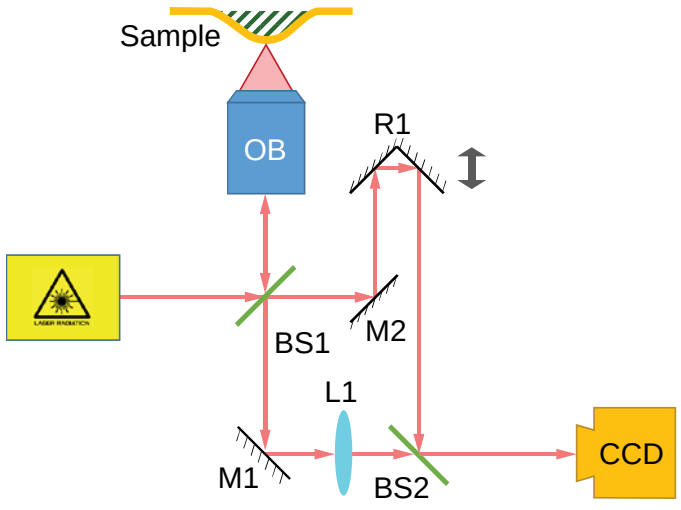

Figure S2. Mach-Zehnder interferometer setup for obtaining the phase information of the

reflected light. A temperature tunable diode laser is used as the light source. The laser incident from the left side is split into two paths when reaches the first beam splitter. One is focused on the sample through an objective, the other acts as a reference light to form the interference pattern. The optical path of the reference arm is adjustable using a retroreflector mounted on a translation stage. The two paths rejoin at the second beam splitter and form the interference fringes on a charge-coupled device. (BS – beam splitter, M – mirror, R – retroreflector, L – lens, OB – objective, CCD - charge-coupled device)

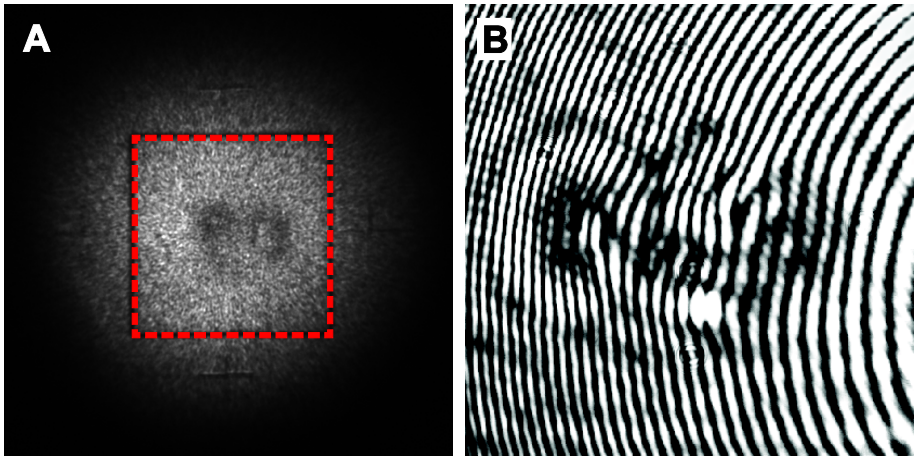

Figure S3. Experimental measurement results for a control sample with the same three-dimensional height profile but without the metasurface. (**A**) A widefield reflection image where the three-dimensional arbitrarily-shaped object is clearly visible. The red dashed box indicates the sample region. (**B**) An interference pattern showing the phase information of the reflected light. We can see that the fringes are distorted in the region of the object. Note that the pattern looks similar to that obtained when the metasurface skin cloak is off (Fig. 3F). This control sample is fabricated on the same chip.

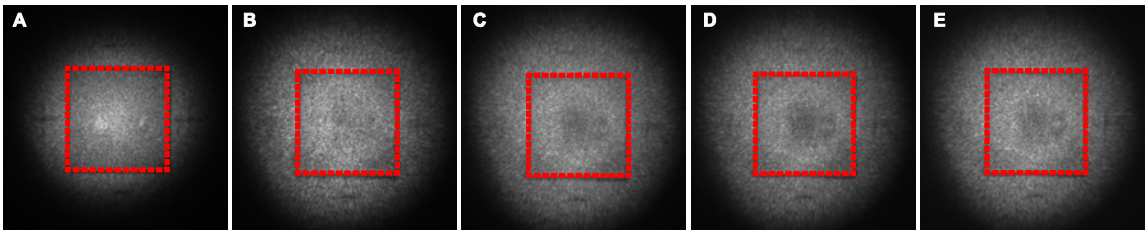

Figure S4. Widefield reflection images for the metasurface skin mask at different wavelengths. (**A**) 710 nm, (**B**) 750 nm, (**C**) 770 nm, (**D**) 790 nm, (**E**) 810 nm. The skin cloak still have some effects, but the performance is getting worse when the wavelength moves further away from the designed one. The sample region is indicated by the red dashed boxes.

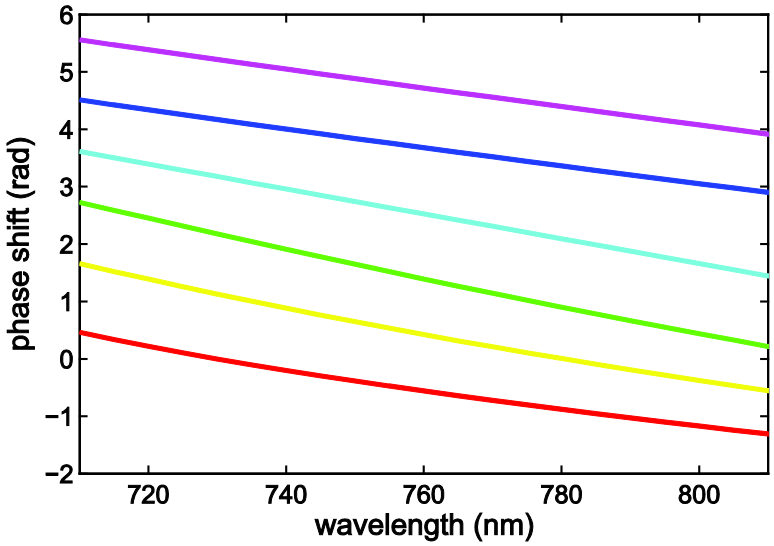

Figure S5. The spectral response of the six nanoantennas. The figure shows the phase shift provided by the nanoantennas versus the wavelength. Each line indicates the response for each antenna design. From bottom to top, the lines corresponding to the antennas with phase shifts of 0, π/3, …, π5/3 at 730 nm. Despite the wavelength change, the (phase shift) separation between each neighboring lines is still approximately the same, with the six antennas roughly covering a 2π phase range. However, the curves are not flat over all the wavelength range – a shorter wavelength has a smaller absolute phase shift. Additionally, the required phase shift is also wavelength-dependent as indicated by Eq. 1. Therefore, the performance of the skin cloak gets worse when the wavelength moves away from the designed one.